Supporting Information

Harnessing the Mechanism of Glutathione Reductase for Synthesis of Active Site Bound Metallic Nanoparticles and Electrical Connection to Electrodes

Daniel Scott, Michael Toney*, and Martin Muzikář*

Department of Chemistry, University of California, Davis, Ca 95616 Davis

*Corresponding Authors

Tel: 530-754-5282

Fax: 530-752-8995

E-mail: mdtoney@ucdavis.edu, mmuzikar@ucdavis.edu

Electrochemical Impedance Spectroscopy Studies of GR and GR-AuNP Immobilized on TGPE The basic principle of electrochemical impedance spectroscopy- (EIS) is the application of a small amplitude sinusoidal excitation signal, usually potential, to the system under investigation and measurement of the sinusoidal current response. EIS is a powerful technique for the characterization of biomaterials such as enzymes, receptors, antigens, antibodies etc.[1] It usually involves formation of the complex between biomaterial immobilized in a monolayer or a thin film on the electrode and the analyte. Formation of such a complex alters the capacitance and resistance of the monolayer-electrolyte or electrode-electrolyte interfaces.

In our study, faradaic EIS was used to monitor GR and GR-AuNP immobilization on the TGPE. In order to measure electrical impedance at the interface, the external redox probe $[Fe(CN)_6]^{3-/4-}$ was added to the electrolyte solution. This probe enables a faradaic current at the electrode surface. Enzyme immobilization results in an effective "insulation" of the electrode surface (by blocking physical access of the probe) and an increase in the charge transfer resistance.

The data analysis in our experiments was based on the Randles equivalent circuit for the interfacial impedance which consists of the solution resistance (R_s), the charge transfer resistance (R_{ct}), the mass transport resistance (Z_{war}) and the constant phase element (CPE).

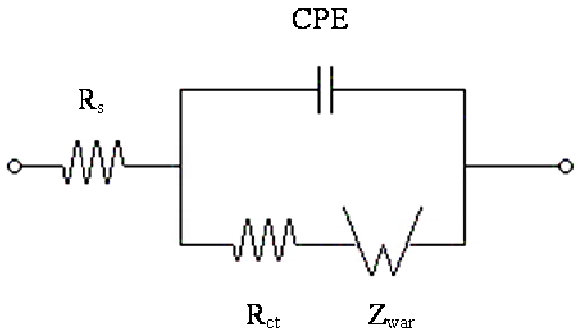

Figure 1. Equivalent circuit of the cell according to Randles: Rs - the solution resistance R_{ct} - the faradaic impedance, Z_{war} - the Warburg impedance, CPE – constant phase element.

The charge transfer resistance data were extracted from Nyquest plots, where the imaginary part of the impedance is plotted as a function of the real part. In most simple cases, the impedance of a modified electrode is controlled by diffusion of the redox probe at lower frequencies and by interfacial electron transfer at higher frequencies. The resulting graph consists of a semicircular region closer to the axis and a diffusional region that linearly increases indefinably. The semicircular region of these data can be fitted to a circle whose diameter represents the value of R_{ct}. R_{ct} increases is proportion to enzyme immobilization (*i.e.* physical obstruction of access to the electrode surface by the probe).

For immobilization of GR itself, TGPE was soaked in the 1.76 μM GR in 100 mM phosphate buffer, pH 7.4 for different amounts of time (30 min, 13 hr, and 24 hr) and the redox probe (10 mM $K_2Fe(CN)_6$) was monitored at 170 mV vs. Ag/AgCl (3M KCl) reference electrode. Similar experiments were performed for electrodes soaked in GR-Au_5, GR-Au_{50}, and GR-Au_{150} for an equivalent amount of time (30 min).

The charge transfer resistance (R_{ct}) increased on the binding of GR to the graphite electrode surface. It resulted in the formation of a barrier that blocked the electron

exchange between the electrode and redox probe in the electrolyte. The value of charge transfer resistance was found by fitting experimental impedance data in the form of a Nyquest plot. The diameter of the semicircle at higher frequencies was taken as R_{ct}.

Figure 2 shows faradaic impedance spectra corresponding to the formation of the GR layer on the graphite electrode surface for times between 30 min and 24 hr. When the enzyme immobilization process proceeded, the semicircle diameter in the impedance plot increased and the heterogeneous rate constant of $[Fe(CN)_6]^{3-/4}$ decreased. Charge transfer resistance of 75 Ω for 30 min GR immobilization time increased to 180 Ω for 24 hr immobilization. It represents a 2.5 fold increase in R_{ct} and a 2.5 fold decrease in $[Fe(CN)_6]^{3-/4}$ electron transfer rate. It can be seen that with longer immobilization time, R_{ct} levels off and approaches a saturation level. Note that the measured R_{ct} corresponds to the formation of an enzyme layer on the electrode, and does not necessarily means that all immobilized enzyme is active.

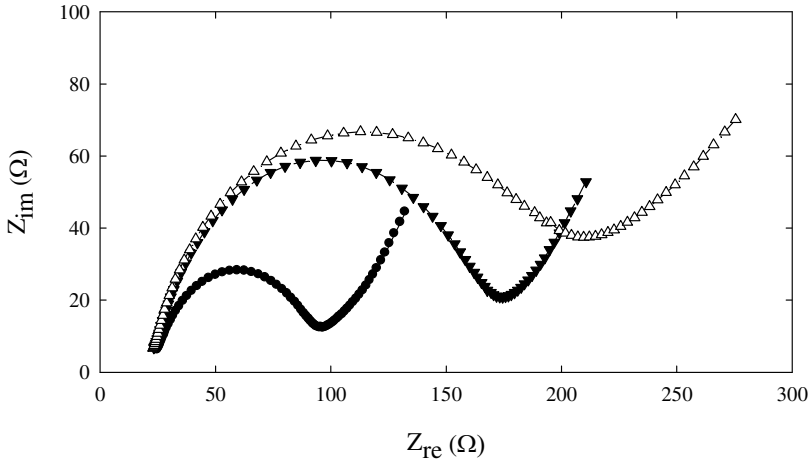

Figure 2. Nyquest plot for 10 mM $Fe(CN)_6^{3-/4-}$ redox probe measured at a redox potential of 0.17 V vs Ag/AgCl (3M KCl) in 100 mM phosphate buffer, pH 7.4, for the immobilization of GR for different amounts of time: 30 min (●), 13 hr (▼), and 24 hr (Δ). Frequency range 0.5 Hz – 20 KHz.

The same technique was used to compare 30 min immobilization of GR, GR-Au_{50} and GR-Au_{150}. The experimental data are shown in Figure 3. Immobilization of GR-Au_{50} and GR-Au_{150} complexes on graphite paper did show an increase in probe R_{ct} compared to GR alone. An R_{ct} of 75 Ω in case of GR increased to 120 Ω in case of GR-Au_{150}. It suggests a 1.5 fold increase of R_{ct} in the presence of the gold nanoparticle. Based on the data in Figures 2 and 3, GR immobilization on the electrode surface would be complete after ~30 hr. It was also demonstrated that GR-AuNP immobilizes to a greater extent on the electrode than GR alone. The amount of immobilization slightly increases with increasing gold nanoparticle size. On the other hand, extent of immobilization is only ~1.5 fold greater compared to an 18 fold increase in the FAD peak currents in CVs for GR-Au_{250}. While impedance data show that more GR is immobilized in 24 hr than GR-Au_{150} in 30 min, there is nonetheless still ~12 fold larger CV currents for GR-Au_{250}.

The results clearly show that the peak current increase for GR-AuNP complexes at the potential of FAD is not caused by greater GR-AuNP immobilization.

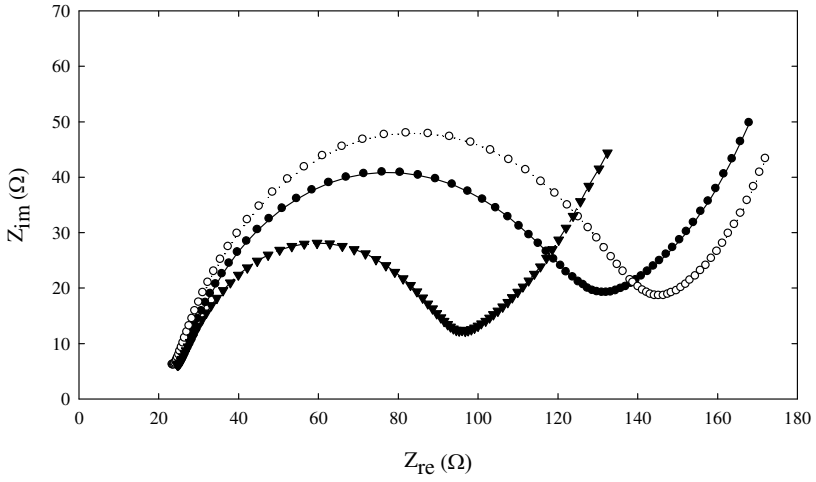

Figure 3. Nyquest plot for 10 mM $Fe(CN)_6^{3-/4-}$ redox probe measured at redox potential of 0.17 V vs Ag/AgCl (3M KCl) in 100 mM phosphate buffer, pH 7.4, for the immobilization of GR (▼), GR-Au_{50} (●), GR-Au_{150} (○) for 30 min. Frequency range 0.1 Hz – 10 KHz.

Direct Determination of TGPE-Bound GR and GR-AuNP The Bio-Rad DC protein assay is a colorimetric assay for protein concentration determination following detergent solubilization. The standard protein assay protocol was used to determine the amount of GR, GR-Au_{50} and GR-Au_{250} immobilized on the TGPE. Preparation of 5 μM GR, GRrAu_{50} and GR-Au_{250} was effected by mixing the appropriate amount of GR, NADPH and $AuCl_4^-$, all in 100 mM phosphate buffer, pH 7.4. Four millimeter diameter TGPE discs were soaked in GR, GR-Au_{50} and GR-Au_{250} buffered solutions for 30 min, then washed with GR-free buffer and stored for colorimetric analysis.

Enzyme immobilized on the TGPE was removed from by boiling in 1% SDS for 30 min. The sample was concentrated to 50 μL and used together with a sample of unimmobilized enzyme for protein assay experiments. A standard calibration curve was

prepared using IgG in the range of 0.015 to 0.3 mg/mL. Both immobilized and unimmobilized enzymes were assayed.

The data do not show a significant difference in the amount of immobilized GR, GR-Au_{50}, or GR-Au_{250} within the estimated measurement error of ~25% (Figure 4).

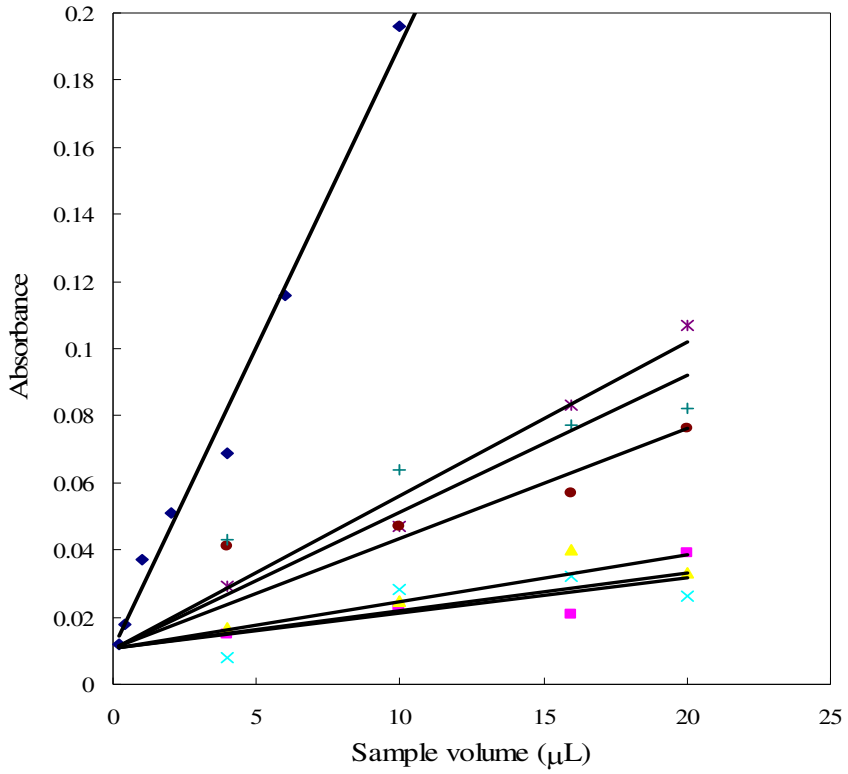

Figure 4. Determination of GR protein concentrations by Bio-Rad DC protein assay. GR-Au_{250} (magenta square), GR (aqua ×), GR-Au_{50} (yellow triangle) immobilized on GPE. GR-Au_{50} (maroon circle), GR-Au_{250} (olive cross), and GR (eggplant ※) in solution. and IgG calibration curve (navy diamond).

Oxidase Activity of the GR-gold Nanoparticle Complex 10, 20 and 40 gold atoms attached to the enzyme increased the rate of NADPH consumption in air equilibrated 100 mM phosphate buffer, pH 7.6, in the absence of Au^{3+} or glutathione. (Figure 6).

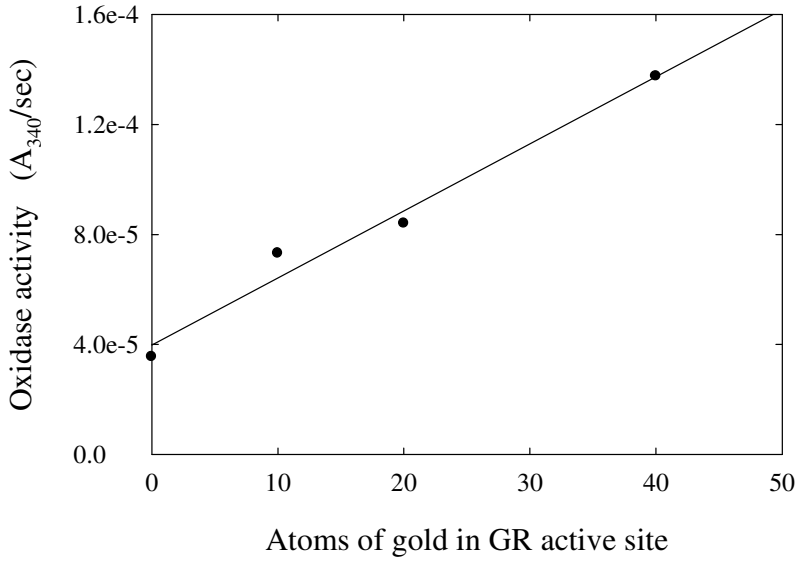

Figure 6. Increase in oxidase activity as a function of the amount of gold attached to the enzyme in air equilibrated 100 mM potassium phosphate buffer, pH 7.6.

Atomic Absorption Spectroscopy of GR Bound Gold There was a small gold background in the AA measurements, possibly due to nonspecific binding of $AuCl_4^-$ to GR or contamination in the samples. However, when GR was allowed to react with $AuCl_4^-$ in the presence of NADPH, GR bound the reduced gold tightly. The GR-bound gold persisted after purification with a size exclusion column. As the stochiometry of $AuCl_4^-$ to GR in the reaction increased, an increase in the measured amount of $AuCl_4^-$ was only observed in the samples that contained NADPH (Figure 7).

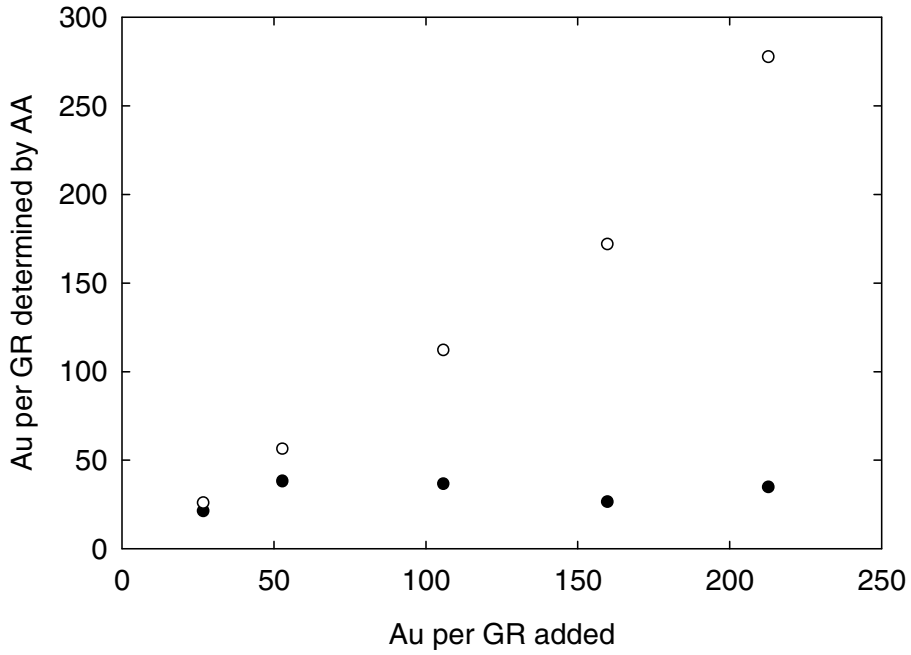

Figure 7. Plot of the number of Au atoms per enzyme observed by AA as a function of the number of Au atoms per enzyme added in the reaction. The plot is for a 30 min incubation of 20 μM GR in 100 mM phosphate buffer, pH 7.6 with (○) and without (●) 3 mM NADPH. Unreacted NADPH and $AuCl_4^-$ in the solution were removed using a Sephadex G25 size exclusion spin column prior to analysis.

SDS-PAGE of GR and GR-AuNP Complexes SDS-PAGE experiments under denaturing conditions reveal that the addition of $AuCl_4^-$ to the enzyme, in the presence of NADPH, result in an increase in the amount of enzyme in the dimeric form (Figure 8). This dimeric form is seen to a small extent in GR without gold as well. 2-Aminoethanethiol removes the nanoparticle from the enzyme. It suggestes that the reduced gold is attached to the enzyme such that it interacts with both of the monomers of the enzyme, stabilizing the dimer. As the 2-aminoethanethiol is increased above 2 mM, the gold nanoparticle is remove from GR, which runs again primarily as a monomer.

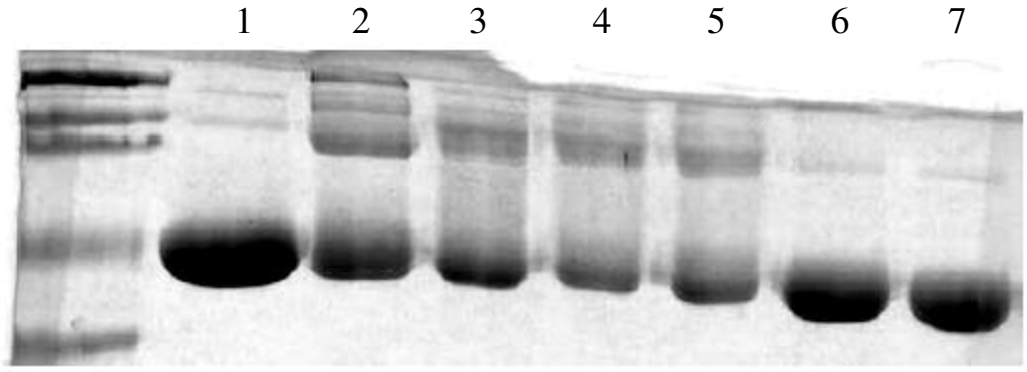

Figure 8. SDS-PAGE of GR and GR-AuNP. (1) GR, (2) GR Cys-tag mutant (not discussed in this work), (3) GR-Au_{18}, (4) GR-Au_{18} in 1 mM 2-aminoethanethiol, (5) GR-Au_{18} in 2 mM 2-aminoethanethiol, (6) GR-Au_{18} in 4 mM 2-aminoethanethiol, (7) GR-Au_{18} in 8 mM 2-aminoethanethiol.

References

(1) Katz, E., Willner, I. *Electroanalysis* **2003**, *15*, 913-47.